

Magnetic coupling of structural microdomains in bcc Fe on Cu(001)

F. Scheurer, R. Allenspach, P. Xhonneux,* and E. Courtens

IBM Research Division, Zurich Research Laboratory, 8803 Rüschlikon, Switzerland

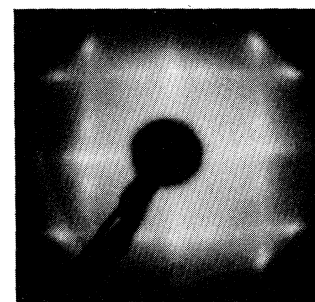
(Received 10 June 1993)

With increasing thickness, thin epitaxial Fe films on Cu(001) undergo a crystallographic transformation beyond ≈ 12 monolayers. Four types of elongated bcc domains are formed, producing the low-energy diffraction pattern previously called (3×1) . The angular-dependent magneto-optical Kerr effect and magnon-light-scattering results indicate that the domains are tightly coupled magnetically, at least between twin pairs. Moreover the scattering length of surface magnons is found to depend strongly on their propagation direction.

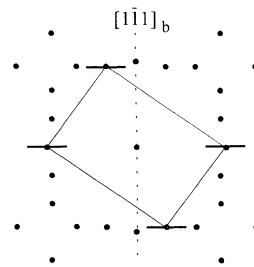
Numerous structural and magnetic studies have been devoted to epitaxial Fe films on Cu(001).¹ These films start their growth as face-centered cubic (fcc), although the stable phase of Fe at room temperature is body-centered cubic (bcc). Recently the one-to-one correspondence between magnetism and the crystallographic structure of Fe/Cu(001) has been stressed.²⁻⁴ With increasing film thickness a succession of at least four different structures is observed by low-energy electron diffraction (LEED) for clean room-temperature growth: (1×1) , (4×1) or (5×1) , (2×1) , and finally a reconstruction that was called (3×1) or pseudo-bcc. The former three are variations on the fcc arrangement. The final structure appears for thicknesses greater than 12 monolayers (ML). Recent analyses⁵⁻⁷ reveal that this structure corresponds to small bcc(110) domains resulting from a phase transition described by Pitsch.⁸ This paper is devoted to structural and magnetic properties of these thicker layers. Surface magneto-optical Kerr-effect (SMOKE) and magnon-light-scattering (MLS) results are presented for Fe film thicknesses between 18 and 25 ML. We will show that the dependence of the signals on the direction of the applied in-plane magnetic field \mathbf{H} proves that the structural domains are not magnetically independent of each other. In fact twin pairs as described by Pitsch⁸ appear to be strongly coupled. This leads to a peculiar angular dependence of the effective anisotropy and also produces a strong directional dependence of the magnon coherence length on spin-wave propagation.

The Fe films were grown by molecular beam epitaxy with perpendicular incidence onto a Cu(001) single crystal kept at room temperature. The experimental setup and all further details concerning preparation and characterization of the films are described in detail in Ref. 4. LEED, MLS, and SMOKE were measured *in situ*, while the angular dependence of the SMOKE signal was determined outside the vacuum system. For the latter, the films were coated with a thin layer (≈ 20 ML) of Cu before being exposed to air. The coating of such thick Fe films with Cu has no effect on the magnon frequencies observed by MLS, and thus does not change the overall magnetic properties of the films. The SMOKE experiment is performed using 632.8-nm laser radiation with the plane of incidence perpendicular to \mathbf{H} . To determine the angular dependence the sample is rotated around its normal.

With increasing film thickness a major change in the LEED patterns occurs between ≈ 12 and ≈ 16 ML. The final pattern is illustrated in Fig. 1 for a 20-ML film. It can be considered to be the superposition of the four possible bcc domains⁵ shown in Fig. 2. For convenience we attach a subscript f to fcc and b to bcc indices, and discuss the particular orientation of domain (a) in Fig. 2. The rectangular reciprocal lattice cell of this patch is reproduced in Fig. 1(b). The remaining LEED spots result from the orientations (b) to (d). Each domain corresponds to a Pitsch transformation in which the rows of nearest-neighbor atoms are preserved, the fcc face diagonals, $[110]_f$, becoming bcc body diagonals, $[1\bar{1}1]_b$.^{8,9} The bulk bcc cell can be obtained from the fcc cell by a distortion combined with a shear. The distortion consists of a



(a)



(b)

FIG. 1. (a) LEED pattern obtained on a 20-ML Fe/Cu(001) film at 180 eV. (b) The theoretical pattern deduced from the domains in Fig. 2. The rectangle shows the centered reciprocal cell corresponding to Fig. 2(a). The direction of the streaks is represented by the short bars. The dotted line indicates the real-space $[1\bar{1}1]_b$ direction.

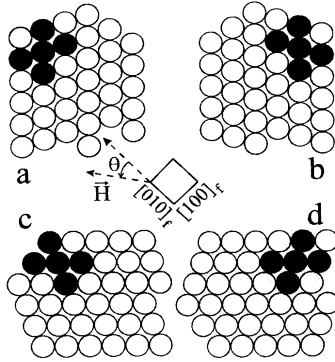


FIG. 2. The four domains of bcc Fe (open circles) on fcc Cu (shaded circles) drawn to scale, each with its bulk lattice constant. The solid circles illustrate the single rectangular unit cells of each domain.

small compression along the $[110]_f$ rows, a large compression perpendicular to the rows along $[1\bar{1}0]_f$, and an expansion perpendicular to the film. The shear is in the $(1\bar{1}0)_f$ plane along the $[110]_f$ direction. Hence this transformation preserves the matching with the substrate reasonably well along the $[110]_f$ rows, but only over short distances in the perpendicular direction, $[1\bar{1}0]_f$. Frequent alternation in the sign of the shear produces twin domains of (a) and (b), or of (c) and (d), respectively. Twinned elongated domains were already observed by Pitsch in the reconstruction of freely suspended austenite films.⁸ From the observed streak direction we conclude that the shorter axis of the patch is perpendicular to the $[1\bar{1}1]_b$ direction, as expected. This qualitative analysis is supported by quantitative LEED results and scanning tunneling microscopy (STM).^{5,6} In particular the size of these domains is less than several hundred angstroms.

Hysteresis curves have been measured by SMOKE as a function of the angle θ made by the in-plane \mathbf{H} field and the $[010]_f$ direction of the substrate, as sketched in Fig. 2. Figure 3 presents a polar plot of the observed coercive field H_c for the magnetization component parallel to the

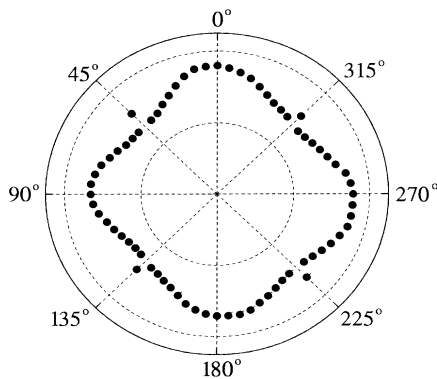


FIG. 3. The coercivity H_c along the in-plane applied field vs its orientation θ , as measured by SMOKE. The equifield line distance is 4 kA/m. The Fe film is 25 ML thick and coated with 20-ML Cu.

TABLE I. Angles of the magnetic anisotropy axes for the four independent domains shown in Fig. 2, with respect to $[010]_f$. The angles are listed over two quadrants, from -90° to $+90^\circ$.

Domain	Easy axis	Medium axis	Hard axes
a	9.7°	-80.3°	64.5° and -45°
b	80.3°	-9.7°	25.5° and -45°
c	-80.3°	9.7°	45° and -25.5°
d	-9.7°	80.3°	45° and -64.5°

applied field. Owing to the size of the light spot (1 mm diam), the measurement represents an average over the four domain orientations. It exhibits quite accurately the fourfold symmetry expected from the symmetry of the fcc substrate. There are four main maxima near $\theta = n \times 90^\circ$ ($n = 0, 1, 2, 3$) and four secondary maxima rotated $\approx 45^\circ$ from the main ones. We note that the secondary maxima are very narrow ($\pm 2^\circ$) and are superimposed on the broad minima of H_c .

The behavior shown in Fig. 3 cannot be explained on the basis of the magnetocrystalline anisotropy of four uncoupled bulk Fe bcc domains, as shown in the following. If we assume the magnetocrystalline anisotropy constants to be similar to those of bulk Fe, we meet in each domain one easy axis of the $[100]_b$ type, i.e., $\langle 100 \rangle_b$, one intermediate $\langle 110 \rangle_b$ axis, and two hard $\langle 111 \rangle_b$ axes. The corresponding angles with respect to the $[010]_f$ direction are listed in Table I. We emphasize that even when \mathbf{H} points in a hard direction the magnetization \mathbf{M} remains in the sample plane owing to the demagnetizing factor. Since the coercivity is largest when the external field points along an easy axis, one anticipates a maximum of H_c when \mathbf{H} is along $\langle 100 \rangle_b$ and a minimum along $\langle 111 \rangle_b$. Therefore, according to Table I, one should observe eight maxima along the $\pm 9.7^\circ + n \times 90^\circ$ directions and four broad minima around $45^\circ + n \times 90^\circ$. This, however, is in contradiction to the actual observations. We emphasize that the discrepancy cannot be resolved by assuming a permutation of easy, intermediate, and hard axes with respect to bulk Fe. A sign reversal of the first-order anisotropy constant can induce such an interchange, as has been observed, e.g., in Fe/W(110) films,¹⁰ but it preserves the position and number of the H_c extrema. Therefore the independent domain model is invalid.

On the basis of the reconstruction explained above it is likely that the pairs of twin domains (a,b) or (c,d) are magnetically coupled. Considering (a) and (b) in Table I, one notices that at $\approx 0^\circ$ the easy direction of (a) can combine with the intermediate direction of (b) to form an average effective easy magnetic axis. Indeed a simplified model shows numerically that the combined magnetocrystalline energy has its minimum at 2° . In the same way the easy direction of (d) combines with the intermediate direction of (c). Moreover the situation of each couple (a,b) and (c,d) is energetically symmetric about $n \times 90^\circ$. This, however, is no longer true near $45^\circ + n \times 90^\circ$. For (c) and (d) that direction is hard and the coupled magnetization will tilt either towards 0° or 90° , depending on the exact alignment of \mathbf{H} . On the oth-

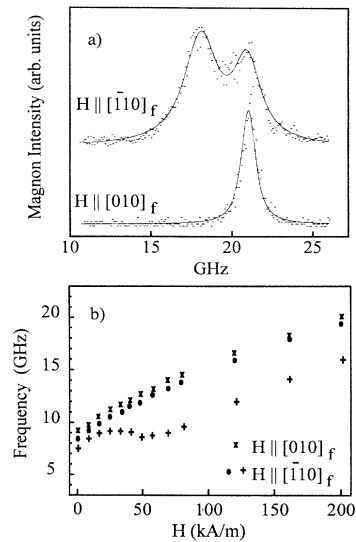


FIG. 4. (a) Magnon spectra obtained for a 25-ML Fe film for $\theta=0^\circ$ ($\mathbf{H} \parallel [010]_f$) and $\theta=45^\circ$ ($\mathbf{H} \parallel [110]_f$), respectively, with $H=200$ kA/m. (b) Magnon frequencies vs applied magnetic field \mathbf{H} for a 18-ML Fe film.

er hand, the couple (a, b) will be in a strongly frustrated situation at $\theta=45^\circ$. The magnetization of (a), \mathbf{M}_a , is pulled towards 9.7° , and the magnetization of (b), \mathbf{M}_b , towards 80.3° , the symmetric position with respect to $\theta=45^\circ$ (see Table I). However, since (a) and (b) are coupled, a motion of \mathbf{M}_a towards 9.7° would imply a motion of \mathbf{M}_b over the hard direction at 25.5° , which is energetically unfavorable. In fact, the angular variation of the independent energies of domains (a) and (b) is strong and of opposite slope near $\theta=45^\circ$. Under such conditions the formation of a small angle between \mathbf{M}_a and \mathbf{M}_b can generate a *local minimum* of the combined energy at $\theta=45^\circ$. Such a local minimum gives rise to an effective intermediate easy axis which produces the very narrow secondary H_c maximum. In particular the width of this minimum depends on the strength of the coupling energy, i.e., on the angle between \mathbf{M}_a and \mathbf{M}_b . The coupling of twin domains is thus able to explain qualitatively all observations made in Fig. 3. It is supported further by the MLS results to be discussed now.

Figure 4(a) shows typical magnon spectra obtained along the two field directions 0° and 45° . For $\theta=0^\circ$, a single sharp peak is observed, whereas for $\theta=45^\circ$, the spectrum becomes much broader and is dominated by two features. The dependence of the magnon frequencies on the applied external field is shown in Fig. 4(b). For $\theta=0^\circ$, it is characteristic for in-plane magnetization with the field applied along an easy axis. For $\theta=45^\circ$, the high-frequency branch is very similar to the one seen at $\theta=0^\circ$. The low-frequency branch, on the other hand, exhibits a dependence that is typical for the field applied in a hard magnetic direction,¹¹ namely with an intermediate minimum at the field value where the static magnetization becomes aligned with \mathbf{H} .

To facilitate the discussion we first consider a case where the domains are large compared to the magnon

wavelength. The above observations are incompatible with four independent domains that would give two peaks for either orientation. At $\theta=0^\circ$ the modes from (a) and (d), or from (b) and (c), would be degenerate by symmetry while at $\theta=45^\circ$, the modes (a) and (b), or (c) and (d), are degenerate. On the contrary, when domains are coupled, the pairs (a, b) and (c, d) are in a symmetric situation and in an easy direction at $\theta=0^\circ$ as explained above. This causes the single narrow peak in Fig. 4(a) and its typical frequency dependence. At $\theta=45^\circ$, the magnetization of the couple (a, b) lies in the frustrated state between the two hard axes at 25.5° and 64.5° , which leads to the high-frequency branch in the $\theta=45^\circ$ spectrum. For the couple (c, d) the field points along a hard direction. This gives the typical behavior of the low-frequency branch with the magnetization becoming aligned with \mathbf{H} at ≈ 50 kA/m. The frequency dependences shown in Fig. 4(b) cannot be derived in the manner of Ref. 4, which did not account for the appropriate anisotropy direction in the bcc films. To perform an approximate calculation, we used the proper anisotropy directions of the single domains to calculate the magnon frequencies, and forced the magnetization into the direction that results from domain coupling. Reasonable agreement with Fig. 4(b) is obtained for $M=830$ kA/m and an anisotropy constant of $K_1=0.25 \times 10^5$ J/m³. The meaning of these effective values, however, is not clear because of the simplicity of the model which is not able to describe the coupling other than phenomenologically.

Actually the domains are considerably smaller than the magnon wavelength observed with MLS (≈ 360 nm) by at least one order of magnitude.^{5,6} At $\theta=0^\circ$, because of the symmetric orientation of both domain pairs, a well-defined magnon wave can propagate without much scattering. This gives the narrow peak observed with MLS. However, at $\theta=45^\circ$, the medium becomes magnetically inhomogeneous and produces broadened features. The observed spectra suggest that sufficient spatial continuity remains for each independent pair of coupled domains, preserving reasonably well-defined magnon frequencies.

We emphasize that the MLS spectra at $\theta=45^\circ$ are extremely sensitive to film preparation. Small differences in growth conditions, unnoticeable with LEED, produce major changes in the shape and splitting of the spectra. We attribute these effects to the microscopic structural arrangement and average size of the domains, as well as to dislocations and defects within the film. A recent theoretical study¹² considers the effect of such imperfections on spin-wave propagation.

In summary, Fe layers on Cu(001) undergo a phase transition from fcc to bcc above ≈ 12 ML. LEED reveals that four types of equivalent, elongated bcc domains coexist. The angular dependences of the SMOKE and MLS signals show that twin domain pairs are strongly magnetically coupled. Although the nature of this coupling is not yet known, exchange is expected to play the key role owing to the small domain size and the short distance between these domains as identified in STM images.⁵ Furthermore the coupling strength depends on the shape of the domains, or more generally on the detailed

morphology of the film. We anticipate that by changing the growth parameters, e.g., substrate temperature or evaporation angle, the arrangement of the domains can be modified. This in turn is expected to modify the details of the magnetic coupling, and hence should be observable in the macroscopic magnetic properties. Finally, the inhomogeneity of the film causes the coherence length of the magnons to depend on the propagation direction. Therefore the system promises to be an interesting one

for the study of spin-wave propagation in inhomogeneous media.

We are grateful to M. Wuttig, H. Neddermeyer, Th. Detzel, and N. Memmel for providing us with copies of their manuscripts prior to publication. The expert technical support of Beat Weiss and Andreas Bischof is gratefully acknowledged.

*Present address: Laboratoire de Physique des Plasmas, Ecole Royale Militaire, 30 av. de la Renaissance, B-1040 Bruxelles, Belgium.

¹For an extensive list of recent references, see Ref. 2.

²J. Thomassen, F. May, B. Feldmann, M. Wuttig, and H. Ibach, *Phys. Rev. Lett.* **69**, 3831 (1992).

³H. Magnan, D. Chandesris, B. Villette, O. Heckmann, and J. Lecante, *Phys. Rev. Lett.* **67**, 859 (1991).

⁴P. Xhonneux and E. Courtens, *Phys. Rev. B* **46**, 556 (1992).

⁵M. Wuttig and J. Thomassen, *Surf. Sci.* **282**, 237 (1993); M. Wuttig, B. Feldmann, J. Thomassen, F. May, H. Zillgen, A. Brodde, H. Hannemann, and H. Neddermeyer, *Surf. Sci.* **291**, 14 (1993).

⁶K. Kalki, D. D. Chambliss, K. E. Johnson, S. Chiang, and R. J. Wilson, *Bull. Am. Phys. Soc.* **38**, 503 (1993).

⁷Th. Detzel, N. Memmel, and Th. Fauster, *Surf. Sci.* **293**, 227 (1993).

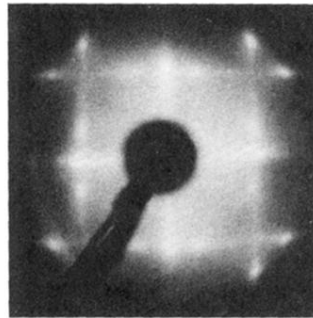
⁸W. Pitsch, *Philos. Mag.* **4**, 577 (1959).

⁹M. Kato, *Mater. Sci. Eng. A* **146**, 205 (1991).

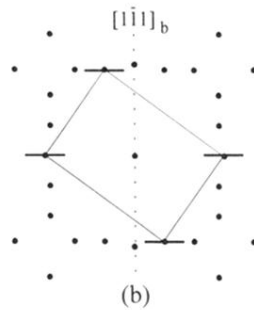
¹⁰U. Gradmann, J. Korecki, and G. Waller, *Appl. Phys. A* **39**, 101 (1986).

¹¹D. Kerkmann, J. A. Wolf, D. Pescia, Th. Woike, and P. Grünberg, *Solid State Commun.* **72**, 963 (1989).

¹²R. L. Stamps, R. E. Camley, B. Hillebrands, and G. Güntherodt, *Phys. Rev. B* **47**, 5072 (1993).



(a)



(b)

FIG. 1. (a) LEED pattern obtained on a 20-ML Fe/Cu(001) film at 180 eV. (b) The theoretical pattern deduced from the domains in Fig. 2. The rectangle shows the centered reciprocal cell corresponding to Fig. 2(a). The direction of the streaks is represented by the short bars. The dotted line indicates the real-space $[\bar{1}\bar{1}]_b$ direction.